

**Figure 1.** Layout of the COR1 instrument package.

Imager (HI) telescopes mounted on the side of the spacecraft. The focus of this paper is the calibration of the inner coronagraph COR1. To distinguish telescopes on the two STEREO spacecraft, either “-A” for Ahead, or “-B” for Behind is appended to the telescope name, e.g. “COR1-A” and “COR1-B”.

The details of the COR1 design are described elsewhere (Howard *et al.* (2008), Thompson *et al.* (2003)). In brief, COR1 is a classic Lyot internally occulting refractive coronagraph (Lyot, 1939), adapted for the first time to be used in space. The instrument layout is shown in Figure 1. Sunlight enters through the front aperture, and is focused onto the internal occulter to remove the direct photospheric light. Because the occulter is mounted onto the field lens, no occulter stem appears in the image. The field lens reimages the front aperture onto a Lyot stop to remove diffracted light, and a series of lenses refocus the coronal light onto a cooled CCD detector. Just in front of the detector is a secondary occulter, known as the focal plane mask, which removes diffracted light from the first occulter. The net effect is that the field of view ranges from 1.4 to 4 solar radii. A bandpass filter restricts the wavelength range to a region 22.5 nm wide, centered on the  $H\alpha$  line at 656 nm.

A Corning Polarcor linear polarizer within the beam allows one to derive both total and polarized brightness. The polarizer is always in the optical path, and is rotated to sample different polarization states. A contrast ratio in excess of 10,000:1 provides completely polarized images to all practical purposes, as was confirmed during ground testing. Three images are taken in rapid sequence at

---

polarizer angles of  $0^\circ$ ,  $120^\circ$ , and  $240^\circ$ . The total brightness  $B$  and polarized brightness  $pB$  can then be derived via these equations

$$B = \frac{2}{3}(I_0 + I_{120} + I_{240}), \quad (1)$$

$$pB = \frac{4}{3}\sqrt{(I_0 + I_{120} + I_{240})^2 - 3(I_0I_{120} + I_0I_{240} + I_{120}I_{240})}, \quad (2)$$

adopted from Billings (1966). Additional equations exist for the angle of polarization.

The following steps are applied to a COR1 image to produce calibrated data. First, a correction is done for certain numerical operations applied on board the spacecraft to keep the data within the valid range of the compression algorithm. Next, a CCD bias derived from the overscan pixels is subtracted, and the data are divided by the exposure time. A flat field image, which includes vignetting effects, is divided into the image. Most of the COR1 field of view is unvignetted, with an essentially flat response. Vignetting occurs near the edge of the occulter, and at the edge of the field stop in the image corners. The flat field image is derived from observations using an opal window built into the aperture door. Finally, the data are multiplied by a calibration factor to convert from data numbers per second ( $\text{DN } s^{-1}$ ) to mean solar brightness (MSB) units. These factors are applied to each of the individual polarization components  $I_0$ ,  $I_{120}$ , and  $I_{240}$  in Equations 1 and 2. Since the polarizer never leaves the beam, but simply rotates about the optical axis, the same calibration factor is used regardless of polarization angle. All of these calibration factors are applied through the IDL routine `SECCHI_PREP` in the SolarSoft library.

Because COR1 is internally occulted, the images are dominated by light scattered from the front objective. To derive useful data, additional steps must be taken to remove the background. The routine `SECCHI_PREP` can be used to remove a model of the background radiation based on trends in the data over the month containing the observation. However, this model background correction will not be considered in the present work. A later paper will explore the COR1 instrumental background correction in more detail.

## 2. Pointing calibration

In order to compare data from the two STEREO spacecraft, the images must first be coaligned. The attitude of the STEREO spacecraft is controlled by a combination of the SECCHI Guide Telescope, the star tracker, and the Inertial Measurement Unit (IMU) (Driesman, Hynes, and Cancro, 2008). The primary sun pointing information comes from the Guide Telescope, which is co-mounted with COR1, COR2, and EUVI on the same optical bench, while the star tracker and IMU mainly control the spacecraft roll. The attitude information embedded within the SECCHI FITS headers is based on a combination of the Guide Telescope telemetry together with attitude history data provided by the STEREO Mission Operations Center (MOC) based on the star tracker and IMU. The MOC also provides ephemeris data about the position of each STEREO spacecraft.

**Table 1.** Changes to the Guide Telescope offset, in arcseconds, since launch on 26 October 2006. Positive x0 is to the right, and positive y0 is upwards.

Date	Ahead		Behind	
	x0	y0	x0	y0
26 Oct. 2006	0.0	0.0	0.0	0.0
21 Dec. 2006	-55.0	55.0		
03 Feb. 2007	0.0	106.3	0.0	69.9
21 Feb. 2007			0.0	-69.9

**Table 2.** Comparison of design versus measured parameters for COR1.

Parameter	Design value	Ahead	Behind
Plate scale (arcsec pixel <sup>-1</sup> )	3.75	3.7522	3.7509
Roll offset (degrees)	0.0	0.204	0.098

Several changes were made during the early commissioning phase to the offset of the Guide Telescope error signal passed to the spacecraft. These changes were made to optimize the performance of the SECCHI telescopes. The history of these pointing changes is shown in Table 1. There is a small effect on the pointing from the angular size of the Sun; the values shown in Table 1 are all normalized to a solar distance of 1 A.U.

From 24–26 February, 2007, the Moon passed in front of the Sun and solar corona (Figure 2). This provided a unique opportunity to establish the absolute pointing of the COR1-B telescope. Circles were fitted to the extremely sharp edges of the Moon’s disk as it moved across the field. This allowed the center position of the Moon to be established to subpixel accuracy. These pixel positions were then compared against the calculated positions of the Moon relative to the Sun as seen by the Behind spacecraft, based on the SPICE ephemerides. Both light travel time and stellar aberration effects were taken into account. By looking at a series of measurements covering the full range of the field of view from left to right, we determined the sun center position, the plate scale, and the roll offset of COR1 relative to the spacecraft. The fitted residual was 3.6 arcseconds, approximately half the (2×2 binned) pixel size used for the measurements.

A similar analysis was performed for COR1-A using the bright star  $\lambda$  Aquarii which passed through the field of view from 28 February–2 March 2007. Here, the fitted residual of 9.1 arcseconds was slightly larger than the 7.5 arcsecond pixel size of the data. Other stars occasionally pass through the fields of view of COR1-A and COR1-B, and are used to monitor the pointing calibration.

Table 2 shows a comparison of the designed and measured parameters for the two COR1 telescopes. The plate scale is for full resolution unbinned images. The default operating mode for COR1 is 2×2 binning to reduce telemetry usage and increase the signal-to-noise. Thus, the normal plate scale is twice that shown in Table 2.

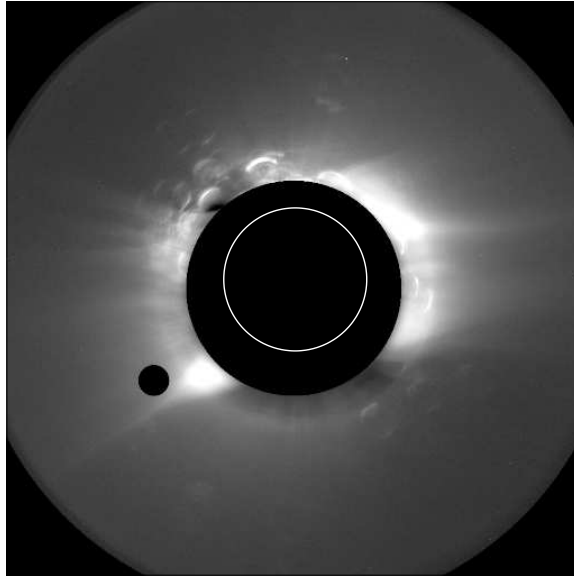


**Figure 2.** Transit of the Moon across the solar corona as seen by COR1-B, 24 February 2007. These images were used to establish the absolute pointing of the COR1-B telescope. The calculated position of the solar disk is shown by the white circle.

In early May 2007 the planet Mercury passed through the fields of view of COR1-A and COR1-B, when the spacecraft were separated by 6.4 degrees (Figure 3). For a few hours on May 3, it was simultaneously visible in both telescopes. This was a unique event—the two spacecraft are now too widely separated for this to occur again. Thus, this was a unique opportunity to test the COR1 pointing calibration. Mercury was overexposed on the COR1 exposures; however the position of Mercury on the images can be established to approximately one pixel accuracy.

The IDL routine `scc_measure` was used to measure the position of Mercury in 3D space, which was then compared against the predicted ephemeris values corrected for light travel time and stellar aberration. The comparison was quite successful. The measured heliographic longitude and latitude of Mercury differed by 0.037 and 0.005 degrees respectively from the ephemeris values, while the distance from the Sun differed by 0.14%. These errors are consistent with an approximately 1 pixel (7.5 arcseconds) uncertainty in the pointing calibration for either telescope, and a 1–2 pixel uncertainty in the co-alignment between COR1-A and COR1-B.

### 3. Radiometric calibration

The initial COR1 calibration was performed in a vacuum tank facility at the Naval Research Laboratory (Howard *et al.*, 2008). These measurements gave preliminary estimates of the conversion factor between detector values of  $\text{DN s}^{-1}$  and MSB (Table 3).

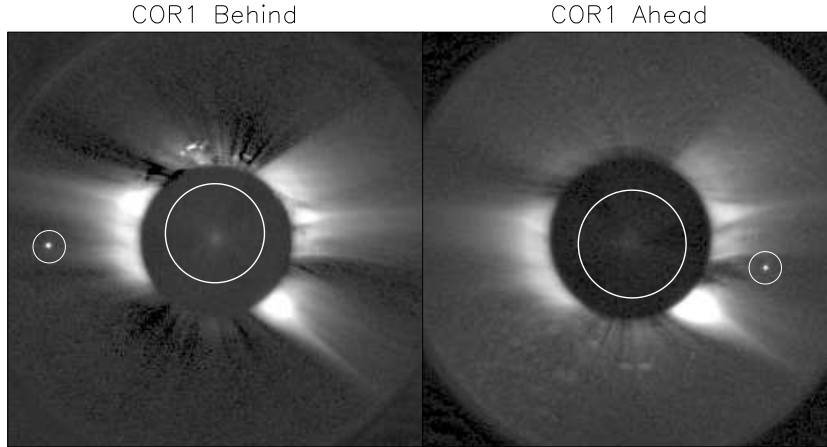


**Figure 3.** Simultaneous observations of the planet Mercury (circled) by COR1-A and COR1-B on 3 May 2007.

Jupiter passed through the COR1-A field of view from 29 November to 2 December 2007 (Figure 4), and through the COR1-B field of view from 15–18 January 2008. Although very bright, the disk of the planet covered several pixels on the detector, and therefore stayed below saturation. The integrated brightness of Jupiter can be modeled as

$$B_J = \pi \left( \frac{R_\odot}{D_\odot} \right)^2 \varpi \left( \frac{R_J}{sD_{sc}} \right)^2 B_\odot, \quad (3)$$

where  $R_\odot$  is the solar radius,  $R_J$  is Jupiter’s radius,  $D_\odot$  and  $D_{sc}$  are the distances from Jupiter to the Sun and the spacecraft respectively,  $\varpi$  is Jupiter’s geometric albedo,  $s$  is the pixel scale in radians, and  $B_\odot$  is the solar brightness ( $B_\odot = 1$ , in MSB units).

Chanover *et al.* (1996) reports the geometric albedo of Jupiter as a function of wavelength. Over the COR1 waveband, the albedo is fairly flat, and has an average value of 0.505. The integrated Jovian brightness is established by taking a small box centered on Jupiter, subtracting a local background, and summing up all the pixels. When these measured brightnesses using the laboratory calibration factors are divided by the model values from Equation 3, the resulting ratios are  $1.0794 \pm 0.0094$  for COR1-A, and  $0.8404 \pm 0.0101$  for COR1-B. Part of the  $\sim 1\%$  uncertainty is a result of the rotation of the planet; since the observations cover several days, all Jovian longitudes are averaged together in the final result. Another error source is a small variation in the modelled flat field due to contamination from scattered light. Applying the above correction factors gives the modified calibration parameters listed in Table 3. The major

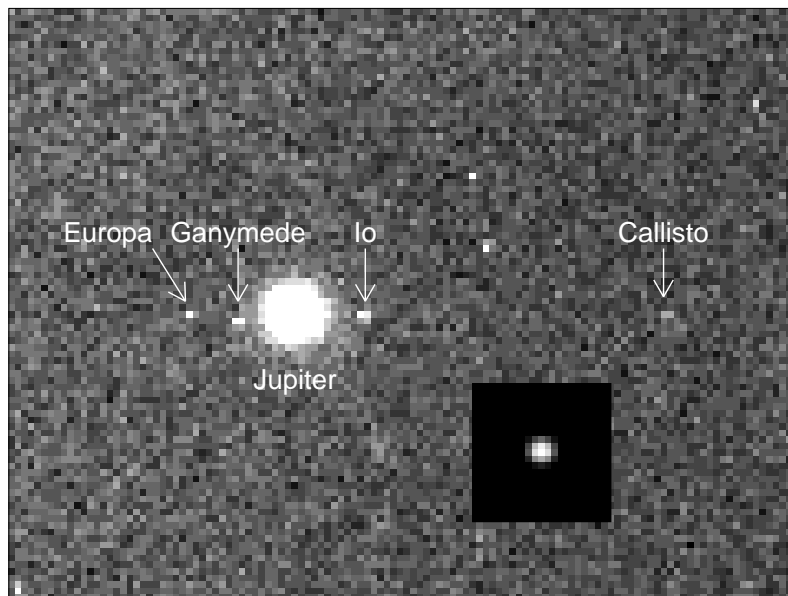


**Figure 4.** Jupiter and its four moons as seen by COR1-A on 2 December 2007. The inset shows the true appearance of Jupiter when not scaled to bring out the moons.

**Table 3.** Comparison of the preflight calibration factors ( $\text{MSB s DN}^{-1}$ ) with those determined from the Jupiter observations.

Telescope	Preflight	Jupiter
COR1-A	$7.10 \times 10^{-11}$	$6.578 \times 10^{-11}$
COR1-B	$5.95 \times 10^{-11}$	$7.080 \times 10^{-11}$

source of uncertainty is in the geometric albedo, which Chanover *et al.* (1996) give as 5–10%.

#### 4. Linearity

The COR1 CCD detector can be operated in two gain modes. The normal mode of operation is to operate the detector at high gain, with about 15 electrons per DN, and with the  $2 \times 2$  pixel summing performed in software. An alternate mode reads out the chip at  $\sim 3.8$  times lower gain, and is used only when summing is performed on the chip. Figure 5 shows the average response in both modes to the opal in the aperture door, as a function of exposure time. The high gain data have been divided by 4 to derive the original signal levels on the CCD before pixel summing. The high gain response is highly linear, with no more than a 1% change in response over the dynamic range. The response at low gain is somewhat less linear, varying by  $\sim 3\%$  over the dynamic range of the detector. Additional tests were made of the instrumental response to scattered light within

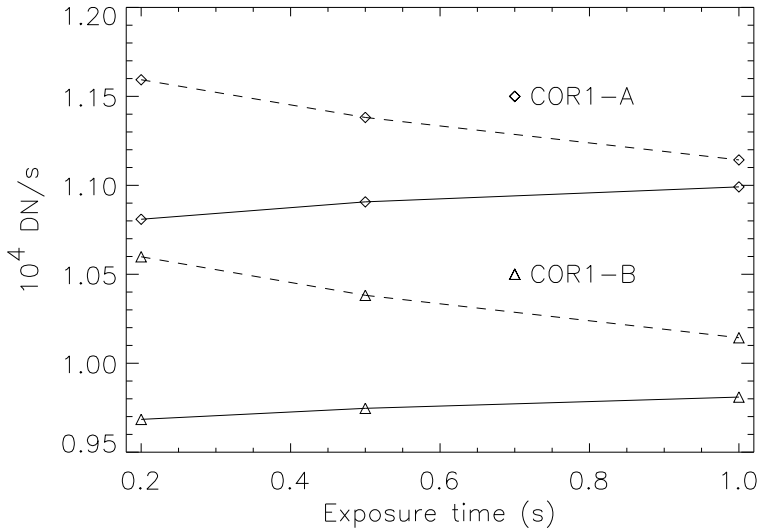


**Figure 5.** Detector response as a function of exposure time. Solid lines are for high gain, and dashed lines are for low gain with onboard pixel summing.

the telescope, which confirmed these results. Since those tests sampled many exposure levels simultaneously within each image, the results shown in Figure 5 cannot be attributed to the shutter.

It was decided to always operate the COR1 detectors in high gain mode, where the response is closer to linear, and always perform pixel summing in software. No attempt is made to remove the small remaining non-linearity in the current calibration software. Because each raw image is dominated by scattered light, only a small fraction of the dynamic range is sampled by any pixel within the image, so the resulting effect on the data is diminished.

## 5. Stability

Whenever either of the STEREO spacecraft performs a momentum dump maneuver, the COR1 aperture door is closed, and measurements are made of the brightness of the opal window. Figure 6 shows the history of the median brightness of the unvignetted portion of the window, normalized to unity for the first set of observations, and corrected for changes in the solar distance. These data provide an indication of the stability of the instrument response. However, since the opal windows are not radiation hardened, they are expected to darken over time. Hence, these measurements provide only an upper limit to the change in the instrument response. The small drops in signal in Figure 6 are consistent with the expected amount of darkening in the opal windows. Therefore, we conclude that COR1 telescopes themselves show little or no change in instrument response.

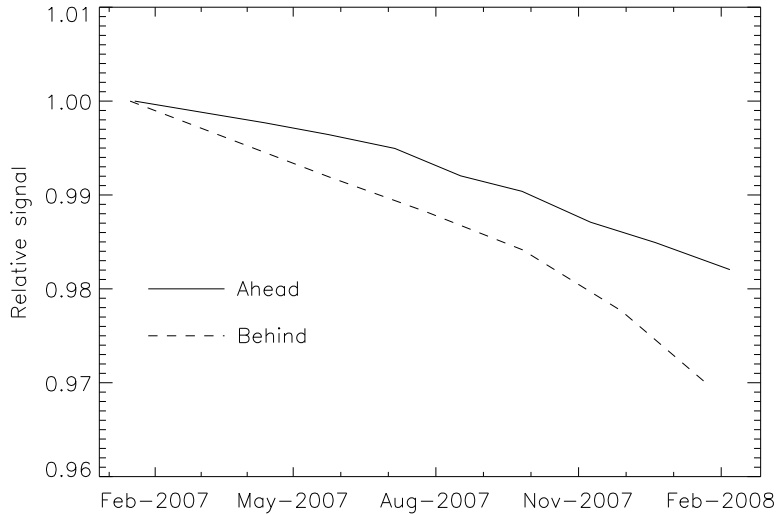


**Figure 6.** Relative brightness of the opal window as a function of time, corrected for solar distance.

## 6. Comparison with other coronagraphs

Figures 7 and 8 show the comparison of the COR1 telescopes with two previously existing coronagraphs. The comparisons are with total brightness for the C2 telescope of the Solar and Heliospheric Observatory (SOHO) Large Angle and Spectrometric Coronagraph (LASCO) (Brueckner *et al.*, 1995), and with polarized brightness for the Mauna Loa Solar Observatory (MLSO) Mk4 K-coronameter (Elmore *et al.*, 2003), since those are the quantities that those coronagraphs respectively observe.

One issue that needed to be addressed to make these plots was background subtraction. As stated before, the raw COR1 data are dominated by instrumental background which needs to be removed to derive useful data. There are automatically generated COR1 background files for any given date available in the SECCHI software. However, these backgrounds are known to include a small amount of the static K-corona. Backgrounds can also be derived from observations made during special spacecraft roll maneuvers, but there are some issues involving the projection of these backgrounds over time that still need to be resolved. This is not a problem for coronal mass ejection (CME) studies, where it is the change in brightness over time which is important, but is a potential issue when comparing observations of the quiescent corona. Small errors in the background subtraction will tend to affect total brightness measurements ( $B$ ) more than polarized brightness ( $pB$ ), since Equation 2 will suppress much of the instrumental background.

In order to have a completely model-free background, it was decided to concentrate on CME observations, and to subtract off a pre-event image to remove

**Table 4.** Observation times in UTC for images shown in Figures 7 and 8. The first time in each telescope column is for the pre-event image, and the second time is for the event image.

Date	COR1-A		COR1-B		C2 or Mk4	
24 Jan. 2007	13:33:00	14:53:00	13:33:06	14:53:06	13:33:21	14:53:46
30 Jan. 2007	09:53:00	10:53:00	09:53:08	10:53:08	09:49:59	10:49:58
09 Feb. 2007	18:53:00	19:53:00	18:53:12	19:53:12	18:56:10	19:55:43

the background, both from the COR1 data, and from the data from the other coronagraphs. The COR1 instrumental background is quite steady, and does not vary significantly on timescales of a day or shorter. For COR1, separate pre-event images were subtracted for each of the three polarized components—the COR1 instrumental background has a polarized component which varies with polarization angle in the same sense as the K-corona. Thus, the background of each polarization component needs to be treated separately. Only events from early in the mission were considered, when the angular separation of the two STEREO spacecraft from each other and from Earth was still small. Event and pre-event images were selected to match observation times as closely as possible. Table 4 shows the times of the selected images. Note that the small difference in time between the Ahead and Behind images is deliberate, to take into account the difference in light travel times from the Sun to each spacecraft.

Coalignment of the images from the various telescopes was done based solely on the information in the FITS headers. The images were then reprojected into a polar representation of position angle and radial distance from Sun center. Figure 7 shows the comparison of COR1 with the LASCO C2 telescope for two strong CMEs that occurred on the 24<sup>th</sup> and 30<sup>th</sup> of January 2007, when the two STEREO spacecraft were only 0.5–0.6 degrees apart. It is evident that the coalignment of the three telescopes is quite good. The LASCO C2 data were reduced using the SolarSoft routine `reduce_level_1.pro`, version 1.45. The bottom two panels show the signal as a function of position angle, averaged between 2.5 and 2.7 solar radii to reduce the noise. All three telescopes follow each other quite closely, with the COR1-A and -B data being practically indistinguishable, and the LASCO C2 data being ~20% lower than COR1.

Another coronagraph that can be compared with COR1 is the MLSO Mk4, which observes the polarized brightness of the corona. Unfortunately, the Mk4 cannot observe 24 hours per day, and did not observe the two strong CMEs used for the LASCO C2 comparison. Instead, we examined a weaker CME observed by the MK4 on 9 February 2007, when the two STEREO spacecraft were separated by 0.7 degrees. The results are shown in Figure 8. Some smoothing has been applied to the Mk4 data to reduce the noise. The general appearance of the CME is the same in all three images, although there may be a slight offset in position angle of the Mk4 data compared with COR1. The Mk4 data are also about 50% higher than COR1, although it is difficult to make a precise one-to-one comparison. There is a small sinusoidal pattern in the Mk4 data which appears to be elevating the values in the region around the CME. In general, though, the COR1 and Mk4 observations agree quite well.

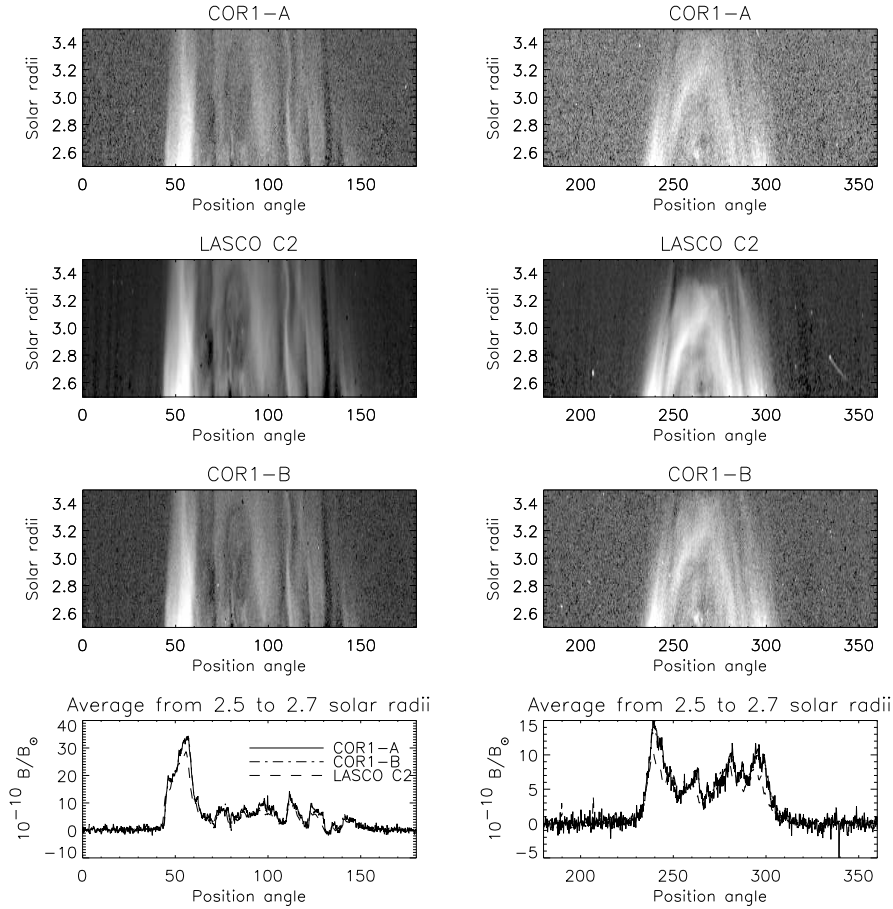


**Figure 7.** Comparison of COR1 total brightness measurements with LASCO C2. The left panels show observations of a CME that occurred on the east limb on 24 January 2007, and the right panels show a CME from 30 January 2007 on the west limb.

## 7. Conclusions

Observations of the planet Mercury demonstrate that the COR1 pointing calibration is good to within one binned pixel (7.5 arcseconds), and that the co-alignment is within 1–2 pixels. The in-flight calibration based on observations of Jupiter agrees well with the pre-flight laboratory calibration, and the cross calibration between COR1-A and COR1-B is confirmed by CME observations made early in the mission, when both spacecraft were along the Sun-Earth line. COR1 measurements of CMEs agree well with those made by LASCO C2 and MLSO Mk4.

Additional work needs to be done to check the COR1 calibration with stellar observations. COR1 does not see the rich collection of stars observed by coronagraphs with larger fields of view, but a few stars do occasionally pass through the field of view. We are working on identifying these stars and determining

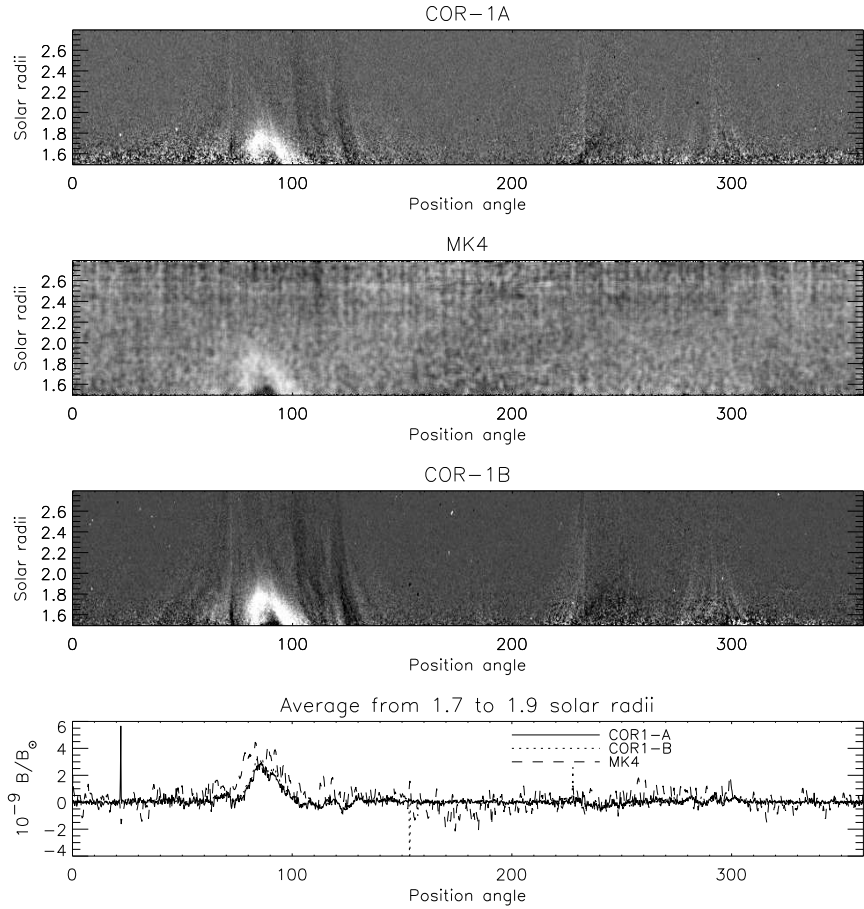


**Figure 8.** Comparison of COR1 polarized brightness measurements with the MLSO Mk4 for a CME on the east limb on 9 February 2007. Some smoothing has been applied to the Mk4 data to reduce the noise.

their brightnesses within the COR1 bandpass. Stars are also used to monitor the pointing calibration.

The SECCHI instrument suite also includes the outer COR2 coronagraph, which observes from 2.5 to 15 solar radii. A future work will cover the intercalibration between COR1 and COR2.

### Acknowledgments

The authors would like to thank Richard Frazin and Joan Burkepile for their help and support in getting this project started, and Joseph Davila and Chris St. Cyr for checking over the manuscript. Chris St. Cyr also pointed us to the Chanover *et al.* (1996) paper. This work was supported by NASA grants NNG06EB68C and NNX07AK209.

---

## References

- Billings D.E.: 1966, *A Guide to the Solar Corona*. New York: Academic Press.
- Brueckner, G.E., Howard, R.A., Koomen, M.J., Korendyke, C.M., Michels, D.J., Moses, J.D., Socker, D.G., Dere, K.P., Lamy, P.L., Llebaria, A., Bout, M.V., Schwenn, R., Simnett, G.M., Bedford, D.K., Eyles, C.J.: 1995, The Large Angle Spectroscopic Coronagraph (LASCO). *Solar Physics* **162**, 357–402. doi:10.1007/BF00733434.
- Chanover, N.J., Kuehn, D.M., Banfield, D., Momary, T., Beebe, R.F., Baines, K.H., Nicholson, P.D., Simon, A.A., Murrell, A.S.: 1996, Absolute reflectivity spectra of Jupiter: 0.25–3.5 micrometers. *Icarus* **121**, 351–360. doi:10.1006/icar.1996.0093.
- Driesman A., Hynes S., Cancro G.: 2008, The STEREO observatory. *Space Sci. Rev.*, in press.
- Elmore D.F., Burkepile J.T., Darnell J.A., Lecinski A.R., Stanger A.L.: 2003, Calibration of a ground-based solar coronal polarimeter. In: Fineschi, S. (ed.), *Polarimetry in Astronomy. Proc. SPIE* **4843**, 66–75.
- Howard R.A., Moses J., Vourlidas A., Newmark J., Socker D., Plunkett S., Korendyke C., Cook J.W., Hurley A., Davila J.M., Thompson W.T., Cyr O.S., Mentzell E., Mehalick K., Lemen J., Wuelsel J., Duncan D., Tarbell T., Wolfson C., Moore A., Harrison R.A., Waltham N.R., Lang J., Davis C., Eyles C., Mapson-Menard H., Simnett G., Halain J., Defise J., Mazy E., Rochus P., Mercier R., Ravet M.F., Delmotte F., Auchere F., Delaboudiniere J., Bothmer V., Deutsch W., Wang D., Rich N., Cooper S., Stephens V., Maahs G., Baugh R., McMullin D.: 2008, Sun Earth Connection Coronal and Heliospheric Investigation (SECCHI). *Space Sci. Rev.*, in press.
- Kaiser M., Kucera T., Davila J., St. Cyr O., Guhathakurta M., Christian E.: 2008, The STEREO mission: An introduction. *Space Sci. Rev.*, in press.
- Lyot, B.: 1939, The study of the solar corona and prominences without eclipses (George Darwin Lecture, 1939). *Mon. Not. Royal Astron. Soc.* **99**, 580–594.
- Thompson W.T., Davila J.M., Fisher R.R., Orwig L.E., Mentzell J.E., Hetherington S.E., Derro R.J., Federline R.E., Clark D.C., Chen P.T.C., Tveekrem J.L., Martino A.J., Novello J., Wesenberg R.P., StCyr O.C., Reginald N.L., Howard R.A., Mehalick K.I., Hersh M.J., Newman M.D., Thomas D.L., Card G.L., Elmore D.F.: 2003, COR1 inner coronagraph for STEREO-SECCHI. In: Keil, S.L., Avakyan, S.V. (eds.), *Innovative Telescopes and Instrumentation for Solar Astrophysics. Proc. SPIE* **4853**, 1–11.

